Food Hydrocolloids 150 (2024) 109721

Contents lists available at ScienceDirect

Food Hydrocolloids

journal homepage: www.elsevier.com/locate/foodhyd

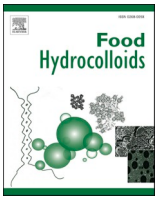

Plant-based bigels for delivery of bioactive compounds: Influence of hydrogel:oleogel ratio and protein concentration on their physicochemical properties

Raquel F.S. Gonçalves [a], Hualu Zhou [c], António A. Vicente [a,b], Ana C. Pinheiro [a,b,*], David Julian McClements [d]

[a] CEB - Centre of Biological Engineering, University of Minho, 4710-057, Braga, Portugal
[b] LABBELS –Associate Laboratory, Braga, Guimarães, Portugal
[c] Department of Food Science and Technology, College of Agricultural and Environmental Sciences, University of Georgia, Griffin, GA, 30223, USA
[d] Department of Food Science, University of Massachusetts, Amherst, MA, 01060, USA

ARTICLE INFO

Keywords:
Hybrid gels
Textural properties
Rheological properties
In vitro digestion
Bioaccessibility
Curcumin

ABSTRACT

Bigels are a class of soft matter systems with high potential in food industry as fortified ingredient replacers or food analogs. The aim of this work was to develop plant-based bigels using potato protein-based hydrogel and candelilla wax-based oleogel. The potato protein concentration and hydrogel:oleogel ratio effects on bigels production was assessed in terms of textural and rheological properties. The incorporation of curcumin and its bioaccessibility after *in vitro* digestion was also evaluated. All samples presented an oleogel-in-hydrogel structure arrangement. Increasing the protein concentration led to increased hardness and G^*, improving the structure and consistency of bigels. The increase of oleogel fraction altered the distribution of oleogel droplets in the hydrogel matrix, affecting the hardness and the consistency of bigels. Overall, the increase of oleogel fraction and protein concentration allowed forming bigels with stronger mechanical properties and higher thermal resistance. The bigel showed a curcumin's bioaccessibility of 16.3 % and a curcumin's stability of 43.8 %, suggesting that this type of structures is promising for the delivery of bioactive compounds at the colon or for slow release of bioactive compounds. Overall, the results showed the possibility to develop potato protein-based bigels with interesting mechanical, rheological and thermal properties by changing the protein concentration and hydrogel: oleogel ratio, expanding the application of bigels in novel food products with high nutritional value and protein content, namely plant-based products.

1. Introduction

Increasing consumers' concerns about the healthiness and sustainability of their diets is leading to a rapid growth in the plant-based food market (Tan & McClements, 2021). For this reason, food researchers are trying to develop plant-based food products with improved physicochemical, functional, sensory, and nutritional properties.

Bigels (also known as hybrid gels) are biphasic systems composed of two different gelled phases, typically a hydrogel and an oleogel (Martín-Illana et al., 2022). These systems can be classified into three types, depending on the spatial distribution of the two phases: oleogel-in-hydrogel type; hydrogel-in-oleogel type; and bi-continuous type (Martín-Illana et al., 2022; Shakeel et al., 2018). Bigels can be designed to exhibit the beneficial attributes of both aqueous and oil phases, such as the ability to incorporate both hydrophilic and lipophilic bioactive compounds in a single system, as well as the possibility of tailoring their physical properties for specific applications by controlling the properties of the individual phases (Fasolin et al., 2021). The main parameters that can impact bigels' properties are hydrogel:oleogel ratio, gelator types and concentrations, and preparation conditions (Fasolin et al., 2021; Okonkwo et al., 2022).

Oleogels are semi-solid systems consisting of a 3D network of organogelators in an organic liquid (Shakeel et al., 2021). The viscoelastic properties of these systems are often thermoreversible – melting when heated above a particular temperature and setting when cooled below a particular temperature (Martín-Illana et al., 2022). The 3D network is

* Corresponding author. CEB - Centre of Biological Engineering, University of Minho, 4710-057, Braga, Portugal.
E-mail address: anapinheiro@ceb.uminho.pt (A.C. Pinheiro).

https://doi.org/10.1016/j.foodhyd.2023.109721
Received 11 September 2023; Received in revised form 21 December 2023; Accepted 29 December 2023
Available online 30 December 2023

typically formed due to the self-assembly of either low-molecular-weight organogelators (LMWOs) or polymeric organic gelators (POGs). LMWOs are able to self-assemble at low concentrations (<2 %) through non-covalent interactions, such as van der Waals forces or hydrogen bonds. Some of the most widely used LMWOS are lecithin, monoglycerides, fatty acids, and natural waxes (Martín-Illana et al., 2022; Shakeel et al., 2021).

Hydrogels are also semi-solid systems, but they consist of a 3D network of polymers that are physically or chemically cross-linked to each other, which can retain high amounts of water through hydration, capillary, and osmotic forces (Martín-Illana et al., 2022). The main gelators used to produced food-grade hydrogels are polysaccharides (e.g., chitosan and alginate) and proteins (e.g., collagen and gelatin) (Okonkwo et al., 2022). Protein-based hydrogels often require that the proteins be denatured prior to their formation, which depends on environmental conditions, such as pH, ionic strength, and temperature (Martín-Illana et al., 2022; Okonkwo et al., 2022). Different biopolymers have been used to formulate the hydrogels in bigels, including k-carrageenan (H. Zheng et al., 2020), starch (Ghiasi & Golmakani, 2022), and alginate (Nutter et al., 2023).

Potato protein is a promising source of functional plant-based ingredients because it is abundant, non-allergenic, and has a high nutritional value (Tan et al., 2023). Potatoes as a whole have a relatively low protein concentration (1.7 %), but potato protein isolates (>90% protein) can be obtained through thermal and acidic coagulation of potato juice after potato starch production (Jiménez-Munoz et al., 2022; Katzav et al., 2020). Potato protein isolate ingredients can be obtained commercially that are composed primarily of patatin, a glycoprotein, protease inhibitors, and high molecular weight proteins (Tan et al., 2023). Potato proteins have been reported to have a high water solubility, as well as good fluid binding, emulsifying, foaming, gelling, and thickening properties (Katzav et al., 2020). However, knowledge of the application of potato proteins as functional ingredients in bigels is currently lacking.

Most previous studies on bigels have focused on pharmaceutical and cosmetic applications, but their interesting properties also make them suitable for food applications such as saturated fat replacers (Ghiasi & Golmakani, 2022; Quilaqueo et al., 2022), 3D printing inks (Xie et al., 2023), plant-based cream analogs (Cui et al., 2022), and fortifiers (Machado et al., 2022). Bigels have already been used as drug delivery systems in pharmaceutical field, showing that they are also promising as bioactive compounds delivery systems for food applications. Bigels can improve the bioactive compound's stability and solubility, protecting them from environmental conditions (e.g., heat, oxygen and pH) during food processing, storage, intake and digestion. Furthermore, bigels can mask off-flavors and textures that some bioactive compounds can present, enhancing the consumer acceptance and intake (Francavilla et al., 2023). Zheng et al. (2020) developed food-grade bigels using κ-carrageenan hydrogel and monoglyceride oleogels to incorporate β-carotene. The increase of oleogel fraction improved the β-carotene stability as well as its *in vitro* gastrointestinal (GI) release. On the other hand, Lu et al. (2022) developed bigels using glycerol monostearate (GMS) oleogel and gelatin hydrogel to co-deliver curcumin and epigallocatechin gallate. The gel structures affected the bioactive compounds release during *in vitro* digestion, where the GMS showed an higher impact on curcumin's release than on epigallocatechin gallate. Bollom et al. (2021) developed bigels using edible lecithin, stearic acid and whey protein to incorporate probiotics and to evaluate its survival during *in vitro* digestion. The authors observed that the developed bigel conferred an effective protection to probiotics against the harsh conditions of the GI tract.

In the current study, we examined their ability to encapsulate curcumin. Curcumin is a hydrophobic yellow-orange polyphenol found in the rhizome of *Curcuma longa* L. and widely applied in the food and pharmaceutical fields because of its beneficial properties (Araiza-Calahorra et al., 2018). It has been used as a natural colorant in food products such as yogurt, ice cream, and cheese, as well as a spice (Almeida et al., 2018; Araiza-Calahorra et al., 2018). Moreover, curcumin has been reported to exhibit several health-promoting properties, such as antioxidant, anti-inflammatory, anti-carcinogenic and anti-proliferative properties (Araiza-Calahorra et al., 2018). The main challenges to incorporating curcumin into foods are its low solubility in aqueous solutions, as well as its degradation when exposed to alkaline conditions, heat, oxygen, and light (Almeida et al., 2018). Furthermore, curcumin exhibits a relatively high rate of metabolic degradation, which leads to the formation of inactive end-products, as well as fast elimination from the body, thereby reducing its oral bioavailability and biological activity (Araiza-Calahorra et al., 2018). Several technologies have been developed to overcome these limitations and improve the bioavailability and activity of curcumin, including encapsulation technologies like nanoparticles (Gonçalves et al., 2021), hydrogels (Zhang et al., 2016), liposomes (Wu et al., 2020), and bigels (Yang et al., 2023).

The main objective of this work was to develop plant-based bigels using potato protein-based hydrogels and candelilla wax-based oleogels to incorporate bioactive compounds. These bigels have the potential to be used as saturated fat replacers, as well as to fortify foods with beneficial nutrients (i.e. higher protein content) and bioactive compounds. The impact of potato protein concentration and hydrogel: oleogel ratio on the formation and properties of the plant-based bigels was assessed, with an emphasis on their structural, textural, and rheological properties. The bioaccessibility of curcumin encapsulated within the bigels after *in vitro* digestion was also evaluated.

2. Materials and methods

2.1. Materials

Corn oil (Mazola, ACH Food Companies, Memphis, TN, USA) was purchased from a local supermarket. Potato protein isolate (Solanic 300, PP-300) was kindly donated by Royal Avebe, U.A. (GK Veendam, Netherlands). All the chemicals and enzymes used in the digestion experiments were purchased from the Sigma-Aldrich Company (St. Louis, MO, USA).

2.2. Bigel production

Oleogels were produced according to Martinez et al. (2021) with some modifications. Candelilla wax (5 %) was completely dissolved in corn oil under magnetic stirring (Isotemp Advanced, Fisher Scientific, USA) at 80 °C and then the hot solution was cooled naturally to room temperature, holding for 24 h.

Hydrogels were prepared according to Zhou et al. (2023) with some modifications. PP-300 was dispersed at different concentrations (15, 20, or 25 %) in distilled water under magnetic stirring (Carrier magnetic stirrer, Bellco Glass Inc., USA) overnight at 4 °C. The protein dispersion was then placed in a water bath at 90 °C for 30 min. The hydrogel formed was cooled to room temperate.

Bigels were obtained as described in Fasolin et al. (2021) and Martinez et al. (2021) with some modifications. The hydrogel was gradually added to the oleogel at room temperature at a ratio of 0.70:0.30 or 0.90:0.10, using an overhead stirrer (Fisher Scientific StedFast Laboratory Stirrer, Model SL1200, USA) operated at 1300 rpm for 10 min. Then, the mixture was subjected to high-speed blending (Bamix®, Switzerland) for 5 min. The samples were then stored at room temperature for 24 h before analysis. The composition of the different formulations tested is presented in Table 1.

2.3. Microstructural analysis

The microstructure of the bigels was observed using confocal scanning laser microscopy with a 40× objective lens (Nikon Eclipse C1 80i, Nikon, Melville, NY, USA) according to Ryu et al. (2023) with some modifications. The instrument's software package (NIS-Elements,

Table 1
Compositions of bigel formulations with different potato protein (PP-300) concentration and hydrogel:oleogel ratio.

Sample	Corn oil ($\%_{w/w}$)	Candelilla wax ($\%_{w/w}$)	PP-300 ($\%_{w/w}$)	Mass Ratio (hydrogel:oleogel)
Bigel_15_70	95	5	15	70:30
Bigel_15_90	95	5	15	90:10
Bigel_20_70	95	5	20	70:30
Bigel_20_90	95	5	20	90:10
Bigel_25_70	95	5	25	70:30
Bigel_25_90	95	5	25	90:10

Nikon, Melville, NY, USA) was used to acquire and analyze the images. The samples were stained with Nile red (10 mg mL^{-1} in ethanol) and FITC (10 mg mL^{-1} in ethanol) to highlight the lipids and proteins, respectively. The sample was placed on a microscope slide, each dye was added, and then the mixture was incubated for 30 s. Any excess dye solution was removed prior to observation.

2.4. Thermal analysis

A differential scanning calorimeter (DSC-250, TA instruments, New Castle, DE, USA) was used to determine the thermal properties of the bigels, hydrogels and oleogel as described by Zhou et al. (2023) with some modifications. A weighed (10–15 mg) sample was sealed in an aluminum hermetic pan. An empty aluminum pan was used as a reference pan. The samples were initially equilibrated at 5 °C and then heated from 5 to 100 °C at 5 °C.min^{-1}. The samples were then held at 100 °C for 15 min before being cooled back to 5 °C at 5 °C.min^{-1}. The onset temperature (T_{onset}), peak temperature (T_{peak}), endset peak (T_{endset}) and enthalpy change (ΔE) were recorded and analyzed using the instrument software (TA Universal Analysis software, TA Instruments, USA). The measurements were performed in triplicate.

2.5. Rheological properties

The rheological measurements were performed as described by Zhou et al. (2023) with some modifications, using a dynamic shear rheometer (HR-20, TA Instruments, New Castle, DE, USA) with a parallel plate geometry (40 mm) and a gap of 1000 μm. A strain test was carried out between 0.01 % and 100 % at a temperature of 25 °C, 50 °C and 80 °C and a frequency of 1 Hz. The viscoelastic properties of the bigels were characterized using shear oscillation measurements in the linear viscoelastic region (LVR). A temperature sweep test was performed by heating the sample from 25 to 80 °C at 3 °C.min^{-1}, holding at 80 °C for 10 min, and then cooled from 80 to 10 °C at 3 °C.min^{-1}. A solvent trap containing water was used to seal the samples from evaporation. A frequency of 1 Hz and strain of 0.5 % was used for these measurements. A frequency sweep was carried out from 0.1 to 10 Hz at 25 °C and a strain of 0.5 %. The dynamic shear moduli were recorded during the different tests. All measurements were performed in triplicate.

2.6. Textural analysis

The texture profiles of bigels were acquired using a texture analyzer (TA.XT Plus, Texture Technologies, Scarsdale, NY, USA) with a T-25 probe (50 mm). A bigel sample (40 g) was formed in a 100 mL cylindrical glass beaker at 25 °C, which led to a sample of 25 mm in height and 45 mm in diameter. A two-compression texture profile analysis (TPA) test was performed with a pre-test speed of 2 mm s^{-1}, followed by a test-speed of 2 mm s^{-1} and post-test speed of 2 mm s^{-1}. The sample was compressed to a distance of 5.0 mm with a trigger force of 5.0 g. After the first compression, the probe was held for 15 s before the second compression was performed. The measurements were carried out in triplicate. The hardness, adhesiveness and cohesiveness were then calculated from the resulting force-distance profiles.

2.7. In vitro digestion

In vitro digestions of curcumin-loaded bigels, curcumin-loaded oleogels, and free curcumin were carried out using the INFOGEST method described by Minekus et al. (2014). This protocol simulates the mouth, stomach, and small intestine phases of the adult human gastrointestinal tract. Briefly, all electrolyte solutions and samples were prewarmed to 37 °C and the enzymes were freshly prepared. The simulated salivary fluid (SSF) was composed of KCl 15.1 mmol.L^{-1}, KH_2PO_4 3.7 mmol.L^{-1}, $NaHCO_3$ 13.6 mmol.L^{-1}, $MgCl_2(H_2O)_6$ 0.15 mmol.L^{-1}, $(NH_4)_2CO_3$ 0.06 mmol.L^{-1} and HCl 1.1 mmol.L^{-1} in Milli-Q water. The simulated gastric fluid (SGF) was composed of KCl 6.9 mmol.L^{-1}, KH_2PO_4 0.9 mmol.L^{-1}, $NaHCO_3$ 25 mmol.L^{-1}, NaCl 47.2 mmol.L^{-1}, $MgCl_2(H_2O)_6$ 0.12 mmol.L^{-1}, $(NH_4)_2CO_3$ 0.5 mmol.L^{-1}, and HCl 15.6 mmol.L^{-1} in Milli-Q water. The simulated intestinal fluid (SIF) was composed of KCl 6.8 mmol.L^{-1}, KH_2PO_4 0.8 mmol.L^{-1}, $NaHCO_3$ 85 mmol.L^{-1}, NaCl 38.4 mmol.L^{-1}, $MgCl_2(H_2O)_6$ 0.33 mmol.L^{-1} and HCl 8.4 mmol.L^{-1} in Milli-Q water.

In the oral phase, SSF, $CaCl_2(H_2O)_2$ 0.3 mol.L^{-1} (0.75 mmol.L^{-1} in the final mixture), and Milli-Q water (to make up the final volume) were added to 5 g of sample. A final ratio of sample to SSF of 1:1 (*w/v*) was targeted. The mixture was incubated at 37 °C for 2 min under agitation (50 rpm), using an incubated tube rotator (Roto-Therm Plus, Benchmark Scientific, Sayreville, NJ, USA).

In the gastric phase, SGF, $CaCl_2(H_2O)_2$ 0.3 mol.L^{-1} (0.075 mmol.L^{-1} in the final mixture), and pepsin solution (activity of 2000 U.mL^{-1} in the final mixture) were added to the previous mixture. The pH was adjusted to 3.0 with HCL (1 mol.L^{-1}) and Milli-Q water was added to make up the final volume. A final ratio of oral sample to SGF of 1:1 (*v/v*) was targeted. The mixture was incubated for 2 h at 37 °C under agitation (50 rpm).

In the intestinal phase, SIF, $CaCl_2(H_2O)_2$ 0.3 mol.L^{-1} (0.3 mmol.L^{-1} in the final mixture), bile salts (10 mmol.L^{-1} in the final mixture), and pancreatin solution (with activity of 100 U.mL^{-1} in the final mixture) were added. The pH was adjusted to 7.0 with NaOH (1 mol.L^{-1}) or HCl (1 mol.L^{-1}) and Milli-Q water was added to make up the final volume. A final ratio of gastric sample to SIF of 1:1 (*v/v*) was targeted. The mixture was incubated for 2 h at 37 °C under agitation (50 rpm). All samples were tested in triplicate.

2.8. Curcumin's bioaccessibility and stability

Curcumin's bioaccessibility and stability were measured after the *in vitro* digestion process according to the method described by Gonçalves et al. (2018), with some modifications. Briefly, 10 mL of digesta was centrifuged (Sorvall Lynx 4000, Thermo Fisher Scientific, Madison, WI, USA) at 18700 *g* at 4 °C for 30 min and the supernatant was collected and assumed to correspond to the micelle phase. Collected whole digesta or micelle phases (5 mL) were mixed with 5 mL of chloroform using a vortex and centrifuged (Sorvall ST 8, Thermo Fisher Scientific, WI, USA) at 700 *g* at room temperature for 10 min. The bottom layer was collected, and the top layer was subjected again to the extraction procedure. The second bottom layer was added to the first layer and analyzed in a UV–VIS spectrophotometer (Genesys 150, Thermo Fisher Scientific, Madison, WI, USA) at 420 nm. Curcumin concentration was determined through a calibration curve of absorbance versus curcumin concentration in chloroform. Curcumin's bioaccessibility was assumed to be the fraction of curcumin inside the micelle phase, while it's stability was assumed to be the fraction of curcumin present in the whole digesta at the end of the digestion (Liu et al., 2018). Therefore, curcumin's bioaccessibility (*B*) and stability (*S*) were calculated using the following equations:

$$B = C_{Micelle} / C_{Digesta} \times 100 \quad (1)$$

$$S = C_{Digesta} / C_{Initial} \times 100 \quad (2)$$

Here, $C_{Micelle}$ and $C_{Digesta}$ are the curcumin concentrations measured at the end of small intestine digestion in the micelle phase and raw digesta, respectively, and $C_{Initial}$ is the curcumin concentration in the sample at the beginning of the digestion process. The effective bioaccessibility (*EB*), which is the combination of the curcumin's bioaccessibility and stability, was calculated using the following equation:

$$EB = B \times S \quad (3)$$

2.9. Statistical analysis

The experiments were performed at least in triplicate and presented as mean ± standard deviation (SD). Statistical analysis was performed using OriginPro 2018 Statistic software (version b9.5.1.195; OriginLab Corporation, Northampton, MA, USA). Data were analyzed using one-way analysis of variance (ANOVA), and Tukey's test was used to evaluate statistically significant differences between the mean values ($p < 0.05$).

3. Results and discussion

3.1. Morphological and microscopy analysis

The bigels were formed with different PP-300 concentrations and different hydrogel:oleogel ratios at room temperature (Table 1). All the bigels had a firm gel-like texture (keeping their original shapes) except for the Bigel_15_70 and Bigel_15_90 samples, which had a softer gel-like structure that collapsed (Fig. 1). The softness of the Bigel_15_70 and Bigel_15_90 samples can be attributed to their low potato protein concentration, which led to the formation of only weak hydrogels. The Bigel_15_70 sample appeared firmer than the Bigel_15_90 one, which was attributed to its higher oleogel fraction (Table 1). Moreover, the CLSM images showed that the oil droplets in the Bigel_15_90 sample were larger and more dispersed than those in the Bigel_15_70 sample (Fig. 1). Regardless of the hydrogel:oleogel ratio or the PP-300 concentration, the CLSM images showed that all the bigels contained spherical oleogel droplets (red) dispersed through a continuous hydrogel matrix (green) (Fig. 1). These results therefore indicated that oleogel-in-hydrogel structures were formed. The oil droplet size tended to decrease with increasing PP-300 concentration, once the increase of PP-300 concentration may have made it more difficult to break down the protein hydrogel phase during the shearing process used to create the bigels, leading to larger hydrogel fragments and smaller oleogel particles. In a related study, Bollom et al. (2020) also reported an increase in hydrogel fragment size in bigel systems at higher whey protein concentrations. Regarding the hydrogel:oleogel ratio, the oleogel particles appeared to be more dispersed in the hydrogel matrix for bigels with a ratio of 90:10 than 70:30, which would be expected to alter the textural and rheological properties of the bigels.

3.2. Textural properties

The textural properties of the different bigels are shown in Fig. 2, where the hardness is the force necessary to obtain an established deformation, the cohesiveness is extent which the sample can be deformed before it ruptures, and the adhesiveness is the required work to pull off the probe from the sample. Bigel_15_70 and Bigel_15_90 had a very weak gel-like structure and therefore it was not possible to proceed with the TPA test. The hardness of the bigels increased with increasing PP-300 concentration, as well as with an increase in the oleogel fraction. Bigel_25_70 was the hardest (16.79 ± 1.95 N) because it had the highest protein concentration and oleogel fraction, while Bigel_20_90 was the softest (3.65 ± 0.17 N) because it had the lowest protein concentration and oleogel fraction. An increase in protein concentration results in a harder hydrogel because there are more structure-forming units within the 3D protein network, thereby strengthening the continuous matrix. Increasing the oleogel fraction leads to more filler particles within the continuous matrix, which is also known to increase the gel strength of composite materials for active fillers (Lupi et al., 2017). These results are in good agreement with the results reported by Zhu et al. (2021). Bigels containing 25 % PP-300 exhibited lower adhesiveness than those with 20 % PP-300. For the bigels containing 25 % PP-300, the adhesiveness tended to increase with increasing oleogel fraction, but these differences were not statistically significant ($p > 0.05$). In contrast, bigels containing 20 % PP-300 exhibited the opposite trend, where the highest value of the adhesiveness was exhibited by the sample with the lower oleogel fraction ($p < 0.05$). These results can be related to the textural properties of the hydrogels produced at the different PP-300 concentrations. During the bigel's production, it was possible to observe that the hydrogels produced with the higher protein concentration were stronger, while those produced with the lower protein concentration, were weaker. Other authors also reported the same tendency (Andlinger et al., 2021). The protein concentration or hydrogel:oleogel ratio did not have a major impact on the cohesiveness values of the bigels, which is in accordance with the results of Zampouni et al. (2023). Overall, however, the protein concentration and hydrogel:oleogel ratio did influence the textural attributes of the bigels. Consequently, it may be possible to create bigels with different textural attributes by controlling these parameters.

3.3. Rheological properties

3.3.1. Frequency sweep

Rheological tests were performed for all bigels to evaluate their viscoelastic properties. Frequency sweeps were carried out in the linear viscoelastic region of the bigels. The tan δ and G^* values measured at 1 Hz are shown in Fig. 3 a) and 3 b), respectively. In general, all bigels had tan δ values lower than 1 but higher than 0.1, which is consistent with a weak gel behavior (Fig. 3 a)). Bigel_15_70 and Bigel_15_90 had the highest tan δ values and lowest G^* values (Fig. 3 a) and b)), indicating that they were the least solid-like, which agree with the visual observations and microscopy analysis in Fig. 1. Despite that, Bigel_15_70 has a

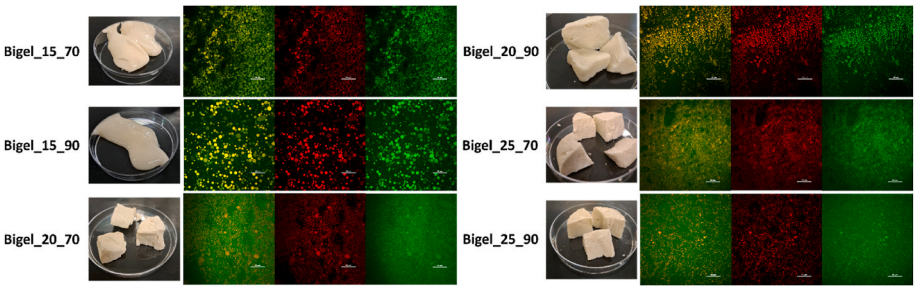

Fig. 1. Photos and CLMS images of bigels with different potato protein concentrations and hydrogel:oleogel ratios. The hydrogel and oleogel are presented as green and red color, respectively.

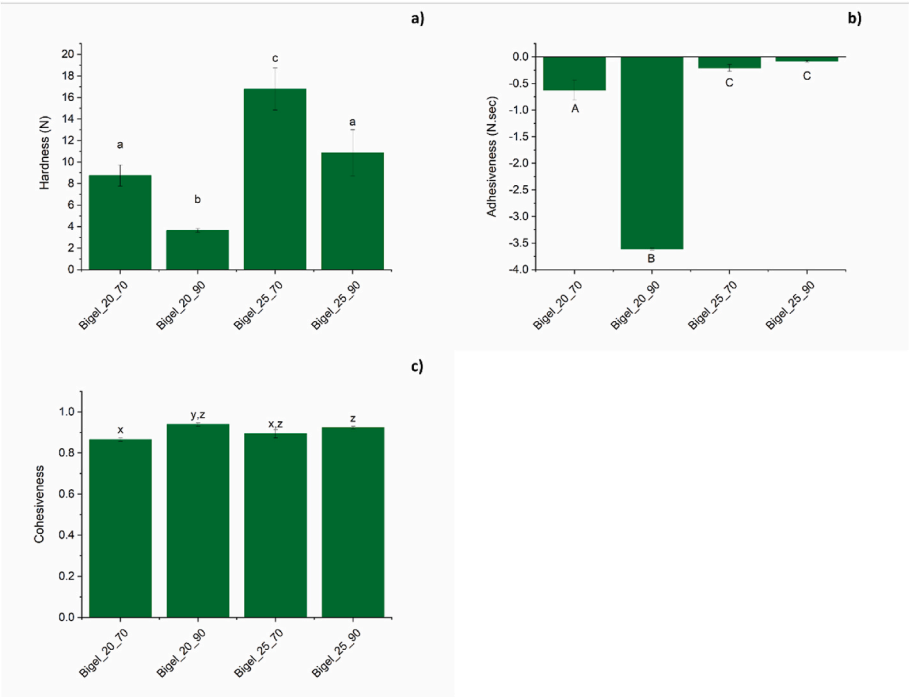

Fig. 2. Textural properties of bigels: a) Hardness; b) Adhesiveness; and c) Cohesiveness. Error bars represent the standard deviation of $n = 3$ replicates. Different letters indicate statistically significant differences ($p < 0.05$).

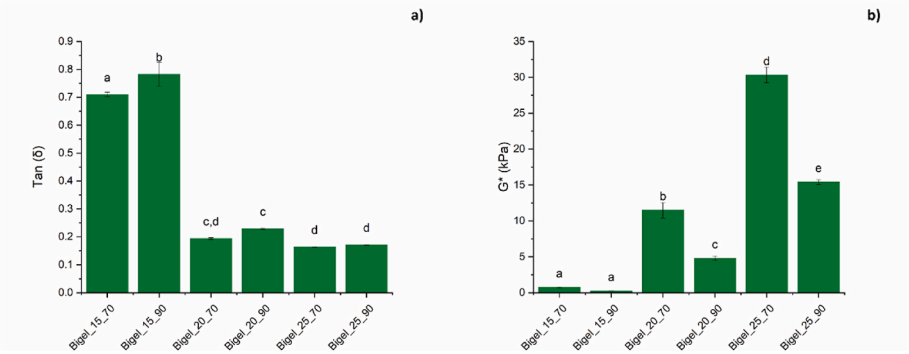

Fig. 3. Frequency sweeps of bigels at 25 °C: a) tan(δ); and b) Complex Modulus (G^*) at 1 Hz. Error bars represent the standard deviation of $n = 3$ replicates. Different letters indicate statistically significant differences ($p < 0.05$).

lower tan δ value than Bigel_15_90, which agrees with the visual observations and microscopy analysis (Fig. 1), which showed that the Bigel_15_70 sample was slightly more structured and the oleogel droplets were in a more compact arrangement. All the other bigels had fairly similar tan δ values, indicating that they were all predominantly solid-like. In contrast, PP-300 concentration and oleogel fraction had a major impact on the G^* values (Fig. 3 b)). An increase in protein concentration or oleogel fraction led to an increase in G^* values. Potato protein hydrogels are mainly formed through non-covalent protein-protein interactions, such as van der Waals, hydrogen bonding, hydrophobic, and electrostatic interactions. Thus, increasing the protein concentration increases the number and strength of the protein-protein interactions, thereby forming hydrogels with a denser and stronger structure (Andlinger et al., 2021). For oleogel-in-hydrogel type bigels, the presence of oleogel particles that act as an active filler is known to increase the elastic modulus (Lupi et al., 2017). As the CLSM images showed, the increase of oleogel fraction contributed to a closer packing of the dispersed phase, improving the bigel consistency. These results are in agreement with those reported in other works (Lupi et al., 2017; Zheng et al., 2020; Zhu et al., 2021). Consistent with the textural analysis, the Bigel_25_70 sample had the highest tan δ and G^* values, thus displaying the strongest mechanical properties. Therefore, an increase of protein concentration or oleogel fraction may produce bigels with stronger mechanical properties.

3.3.2. *Temperature ramp*

The thermal properties of the bigels were characterized using a heating/cooling ramp (Fig. 4). For all bigels, G* values decreased and consequently tan δ increased with the rising of temperature, which can be attributed to thermally-induced softening of the systems. At heating stage, the decrease of bigel strength started from around 30 °C, which is close to the T_{onset} of melting peak obtained on DSC analysis, Table 2. With the exception of Bigel_15_70 and Bigel_15_90, all the samples showed tan δ lower than 1 for all temperatures, indicating a predominantly elastic-like behavior, Fig. 4b) and c), showing the impact of the hydrogel structure on this behavior. Similar results were reported by Zheng et al. (2020) for κ-carrageenan hydrogel-monoglyceride oleogel bigels. Regarding tan δ, the increase of protein concentration decreased

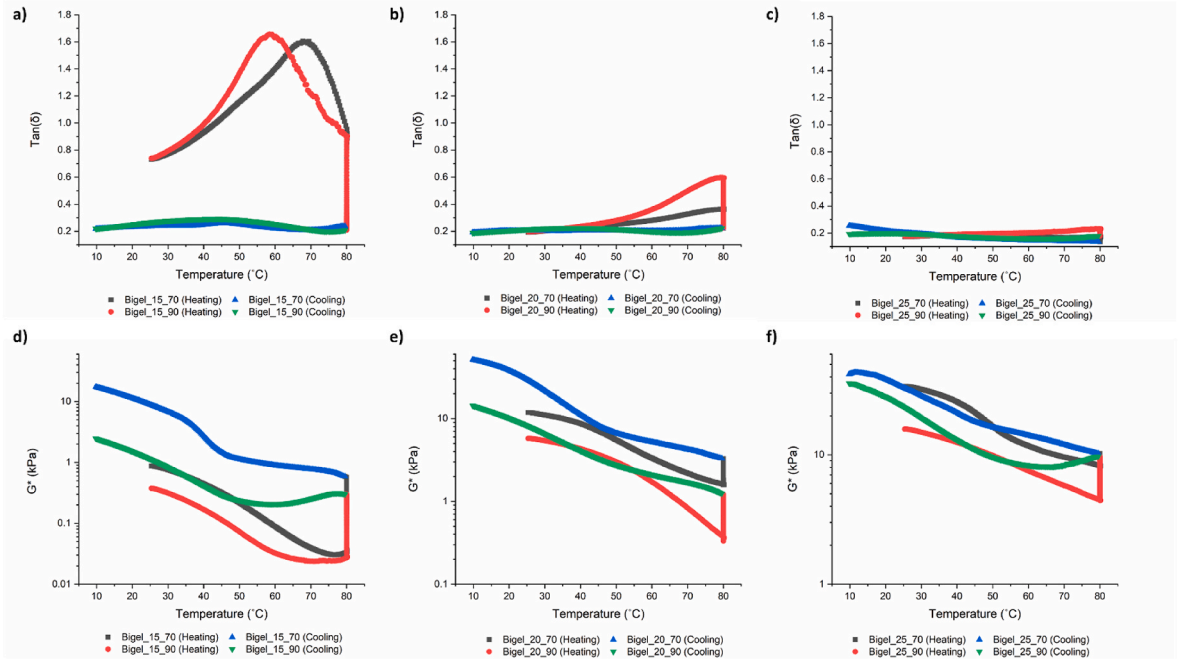

Fig. 4. Rheological properties of bigels as a function of temperature: a-c) tan(δ); and d-f) Complex Modulus (G^*).

Table 2
Thermal properties of bigels, hydrogels and oleogel.

	Bigel_15_70	Bigel_15_90	Bigel_20_70	Bigel_20_90	Bigel_25_70	Bigel_25_90	PP_300 15 %	PP_300 20 %	PP_300 25 %	Oleogel
Melting Temperature										
T_{Onset} (°C)	32.4 ± 2.0^{a}	32.9 ± 1.3^{a}	31.81 ± 0.71^{a}	29.86 ± 4.50^{a,d}	23.98 ± 0.01^{b,d}	ND	58.11 ± 0.07^{c}	57.62 ± 0.14^{c}	57.71 ± 0.16^{c}	25.98 ± 1.15^{d}
T_{Peak} (°C)	42.76 ± 0.42^{a,b}	42.9 ± 1.6^{a,b}	45.6 ± 1.1^{a}	44.76 ± 1.14^{a}	40.53 ± 2.67^{b}	ND	67.37 ± 0.06^{c}	67.02 ± 0.06^{c}	67.20 ± 0.05^{c}	42.39 ± 0.97^{a,b}
T_{Endset} (°C)	51.64 ± 0.93^{a,c,e}	50.4 ± 1.3^{a,e}	59.45 ± 0.51^{b,c}	56.04 ± 2.79^{c}	54.64 ± 4.16^{a,c}	ND	74.59 ± 0.15^{d}	74.36 ± 0.07^{d}	73.97 ± 0.13^{d}	49.44 ± 1.28^{e}
ΔH (J/g)	1.04 ± 0.44^{a,b}	0.36 ± 0.16^{a}	1.20 ± 0.07^{b}	0.34 ± 0.08^{a}	1.52 ± 0.07^{b}	ND	1.82 ± 0.06^{b,c}	2.58 ± 0.03^{c,d}	3.14 ± 0.07^{d}	6.14 ± 0.72^{e}
Crystallization Temperature										
T_{Onset} (°C)	42.51 ± 0.55^{a}	43.2 ± 1.1^{a,c}	41.42 ± 0.37^{a,b}	39.87 ± 0.89^{b}	44.57 ± 0.30^{c}	ND	ND	ND	ND	42.85 ± 0.02^{a,c}
T_{Peak} (°C)	33.36 ± 0.09^{a}	33.79 ± 0.37^{a}	32.21 ± 0.09^{a,b}	32.39 ± 0.38^{a,b}	30.2 ± 2.3^{b}	ND	ND	ND	ND	37.01 ± 0.04^{c}
T_{Endset} (°C)	23.95 ± 0.36^{a}	24.24 ± 0.76^{a}	18.06 ± 0.89^{b}	20.71 ± 0.41^{c}	13.76 ± 0.68^{d}	ND	ND	ND	ND	27.38 ± 0.15^{e}
ΔH (J/g)	1.69 ± 0.23^{a}	0.54 ± 0.08^{b}	1.43 ± 0.13^{a,c}	0.48 ± 0.05^{b}	1.30 ± 0.12^{c}	ND	ND	ND	ND	7.46 ± 0.14^{d}

T_{onset} – Onset temperature; T_{peak} – peak temperature; T_{endset} – endset temperature; ΔE – enthalpy change; ND – Non defined. $^{a–d}$ Mean values with different superscript letters within the same line are significantly different from each other ($p < 0.05$).

the slope of the heating ramp, showing that the bigels with higher protein concentrations were more solid-like and had less thermally-induced structural changes, Fig. 4). Both Bigel_15_70 and Bigel_15_90 presented a tan δ decrease from around 55 °C and 65 °C, respectively, to 80 °C during the temperature holding, showing an increase of the gel strength, Fig. 4a). This suggests that the gel network become stronger, probably due to the unfolding and aggregation of proteins that remained folded during the hydrogel preparation. During cooling, all bigels presented similar tan δ values, showing a solid-like behavior, which can be related to the oleogel crystallization. The G* values of all bigels increased during the cooling, with a step raise from 40 °C, which corresponds to the T_{onset} of crystallization peak on DSC analysis (Table 2), suggesting that the gel structure was recovered. Furthermore, at 25 °C in the cooling sweep, Bigel_15_70 and Bigel_20_70 showed G* values higher than those presented at the beginning of the heating sweep (Fig. 4d and e), indicating that they present a higher consistency after the cooling stage. Similar finding was reported by Martins et al. (2023) on bigels composed by carrageenan/locust bean gum hydrogel and glyceryl monostearate oleogel. Furthermore, the bigels with higher oleogel fraction presented higher increase on tan δ and G* values during heating and cooling stages respectively, showing that the oleogel fraction has high impact on the structure and consistency of bigels during heating/cooling ramp, Fig. 4.

Overall, protein concentration and oleogel fraction had a major impact on the thermal properties of the bigels. Consequently, the thermal behavior of these bigels may be tailored for specific food applications by optimizing their composition.

3.4. Thermal transitions

The thermal transitions observed in the bigels, hydrogels and oleogel during heating and cooling were evaluated by DSC and the results are

shown in Table 2. The potato protein presented an endothermic peak around 74 °C, which was attributed to the thermal denaturation of the globular proteins, forming the hydrogel. Furthermore, during the cooling, the potato protein samples did not show any peak, suggesting that the proteins are irreversibly thermally denatured. Other reports corroborated with these results (Ryu & McClements, 2024; Zhou et al., 2023). All bigels presented no significant differences in melting temperature peak, which corresponds to the candelilla wax melting in the oleogel (42 °C). These results suggest that the thermal behavior of the oleogel did not change after it was mixed with the hydrogel. Bigel_15_70 (1.04 J g^{-1}), Bigel_20_70 (1.20 J g^{-1}) and Bigel_25_70 (1.52 J g^{-1}) had melting enthalpies (ΔH) that were appreciably higher than Bigel_15_90 (0.36 J g^{-1}) and Bigel_20_90 (0.34 J g^{-1}), which can be attributed to the fact the former three bigels contained 30% organogel phase, whereas the latter ones only contained 10%. Our results are consistent with those reported on previous studies of bigels (Yang et al., 2022; Zheng et al., 2023). For Bigel_25_90, it was not possible to identify the melting temperatures of the organogel phase, which may have been due to the high protein concentration in the hydrogel phase. The hydrogel formed by high PP-300 concentrations probably presents a compact network and therefore the thermal behavior of the oleogel fraction did not affect the bigel's thermal behavior. This suggested that higher PP-300 concentrations may turn the bigel more thermally resistant. These results corroborated the thermodynamic properties of bigels presented before. These results are consistent with the thermal rheology properties of the bigels discussed earlier. During the cooling process, the bigels exhibited a crystallization peak (~ 33 °C) that was slightly lower than the that of the oleogel alone (~ 37 °C), but this different was not statistically significant ($p > 0.05$). The crystallization enthalpies exhibited the same tendency as the melting enthalpies, where the bigels with the higher oleogel fractions had higher enthalpies, as would be expected.

Overall, both the protein concentration and oleogel fraction impacted the thermal transitions of the bigels, as shown by the differences in the thermal transition temperatures and enthalpies.

3.5. Curcumin's bioaccessibility and stability

For the gastrointestinal studies, the Bigel_20_70 sample was selected to incorporate curcumin because it formed bigels that could maintain their structure (Fig. 1). A fixed amount (0.05 %) of curcumin was incorporated into the oleogel phase of the bigels and into pure oleogels, for the sake of comparison. Distilled water was then added to the pure oleogel samples so that they contained the same curcumin concentration and oleogel content as the Bigel_20_70 samples. Curcumin bioaccessibility and stability values as well as effective bioaccessibility were then assessed at the end of *in vitro* digestion (Fig. 5). The pure oleogel had the highest curcumin bioaccessibility ($p < 0.05$) followed by the Bigel_20_70 and then free curcumin: 49.1 ± 4.9 %, 16.3 ± 3.9 % and 15.2 ± 2.3 %, respectively. The relatively low bioaccessibility for the Bigel_20_70 sample suggests that the presence of the hydrogel phase inhibited the adsorption of lipase to the surfaces of the oleogel droplets, thereby reducing lipid hydrolysis and curcumin release/solubilization. Conversely, the Bigel_20_70 sample exhibited the highest curcumin stability ($p < 0.05$), which suggests that the hydrogel phase protected the curcumin from chemical degradation. Therefore, the Bigel_20_70 showed the highest effective bioaccessibility followed by free curcumin and pure oleogel, with values of 7.11 ± 1.52 %, 3.38 ± 0.54 % and 3.17 ± 0.66 %, respectively ($p < 0.05$). Jiménez-Munoz et al. (2022) reported some resistance to protein digestion by the potato protein gel at the gastric phase, probably due to the matrix structure complexity, hindering the diffusion of gastric fluids and pepsin in the matrix. They also reported that the protein hydrolysis of potato protein gels occurred mostly in the intestinal phase. Therefore, the low curcumin bioaccessibility and high curcumin stability may be caused by this restriction of hydrogel digestion, which hindered lipid digestion and curcumin release.

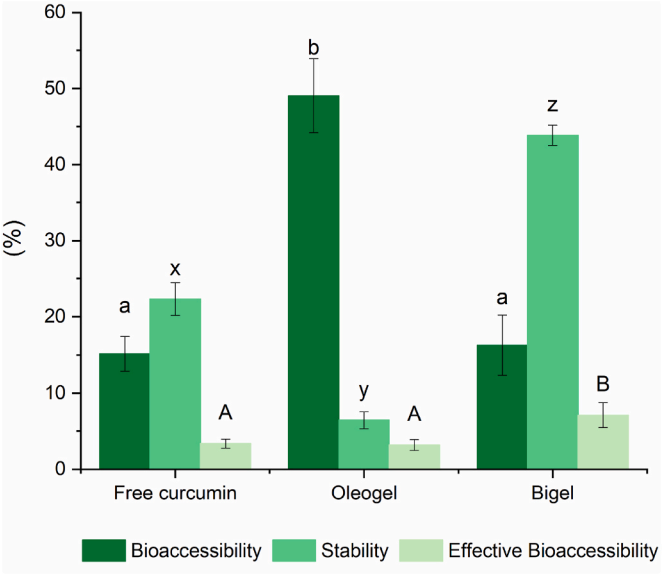

Fig. 5. Bioaccessibility, stability and effective bioaccessibility of free curcumin, curcumin-loaded in oleogel and curcumin loaded in Bigel_20_70 after *in vitro* digestion process. Error bars represent the standard deviation of n = 6 replicates. Different letters indicate statistically significant differences between structures in each parameter ($p < 0.05$).

In conclusion, the bigel structures may be promising for applications where slow release of bioactive compounds or delivery of bioactive compounds to the colon are required.

4. Conclusions

In this study, plant-based bigels were developed using potato protein/water hydrogels and candelilla wax/corn oil oleogels. The influence of protein concentration and hydrogel:oleogel ratio on the bigel properties was evaluated. Regardless of the protein concentration and hydrogel:oleogel ratio, all bigels had an oleogel-in-hydrogel structure. An increase in protein concentration increased the hardness of the bigels. The hydrogel:oleogel ratio also influenced the texture and rheology of the bigels, with the hardness increasing with increasing oleogel content, which was attributed to the ability of the oleogel droplets to act as active fillers in the hydrogel matrix. Thus, the textural attributes of the bigels could be tailored for different applications by controlling their compositions. Encapsulation of curcumin within bigels reduced its bioaccessibility compared to in oleogel alone, but it improved its chemical stability. These effects were attributed to the ability of the hydrogel to inhibit the digestion of the oleogel and the release of the curcumin. Consequently, these bigels may be promising for the encapsulation and delivery of bioactive compounds to the colon or when slow release of bioactive compounds is desirable.

In conclusion, this study suggests that it is possible to produce bigels with interesting mechanical, rheological, and thermal properties, using only plant-based ingredients, in particular potato protein hydrogels. By changing the protein concentration and hydrogel:oleogel ratio, it is possible to tune the bigels characteristics, expanding their application in different plant-based foods. Therefore, the developed bigels have a great potential as a food/ingredient replacers (e.g. decreasing the saturated fat content) or for fortification of plant-based food products, improving their nutritional and functional value, by the increase of the protein content and by the incorporation of bioactive compounds.

CRediT authorship contribution statement

Raquel F.S. Gonçalves: Writing – review & editing, Writing –

original draft, Validation, Methodology, Investigation, Formal analysis, Conceptualization. **Hualu Zhou:** Writing – review & editing, Methodology. **António A. Vicente:** Writing – review & editing, Supervision, Project administration, Funding acquisition. **Ana C. Pinheiro:** Writing – review & editing, Validation, Supervision, Project administration, Funding acquisition, Conceptualization. **David Julian McClements:** Writing – review & editing, Validation, Supervision, Project administration, Funding acquisition, Conceptualization.

Declaration of competing interest

The authors confirm that they have no conflicts of interest with respect to the work described in this manuscript.

Data availability

Data will be made available on request.

Acknowledgments

Raquel F. S. Gonçalves acknowledge the Foundation for Science and Technology (FCT) for her fellowship (SFRH/BD/140182/2018).

This study was supported by the Portuguese Foundation for Science and Technology (FCT) under the scope of the strategic funding of UIDB/04469/2020 unit, and by LABBELS – Associate Laboratory in Biotechnology, Bioengineering and Microelectromechanical Systems, LA/P/0029/2020.

References

Almeida, H. H. S., Barros, L., Barreira, J. C. M., Calhelha, R. C., Heleno, S. A., Sayer, C., Miranda, C. G., Leimann, F. V., Barreiro, M. F., & Ferreira, I. C. F. R. (2018). Bioactive evaluation and application of different formulations of the natural colorant curcumin (E100) in a hydrophilic matrix (yogurt). *Food Chemistry, 261*, 224–232. https://doi.org/10.1016/j.foodchem.2018.04.056

Andlinger, D. J., Bornkeßel, A. C., Jung, I., Schröter, B., Smirnova, I., & Kulozik, U. (2021). Microstructures of potato protein hydrogels and aerogels produced by thermal crosslinking and supercritical drying. *Food Hydrocolloids, 112*, Article 106305. https://doi.org/10.1016/J.FOODHYD.2020.106305

Araiza-Calahorra, A., Akhtar, M., & Sarkar, A. (2018). Recent advances in emulsion-based delivery approaches for curcumin: From encapsulation to bioaccessibility. *Trends in Food Science & Technology, 71*, 155–169. https://doi.org/10.1016/j.tifs.2017.11.009

Bollom, M. A., Clark, S., & Acevedo, N. C. (2020). Development and characterization of a novel soy lecithin-stearic acid and whey protein concentrate bigel system for potential edible applications. *Food Hydrocolloids, 101*, Article 105570. https://doi.org/10.1016/j.foodhyd.2019.105570

Bollom, M. A., Clark, S., & Acevedo, N. C. (2021). Edible lecithin, stearic acid, and whey protein bigels enhance survival of probiotics during in vitro digestion. *Food Bioscience, 39*, Article 100813. https://doi.org/10.1016/j.fbio.2020.100813

Cui, H., Tang, C., Wu, S., Julian McClements, D., Liu, S., Li, B., & Li, Y. (2022). Fabrication of chitosan-cinnamaldehyde-glycerol monolaurate bigels with dual gelling effects and application as cream analogs. *Food Chemistry, 384*, Article 132589. https://doi.org/10.1016/j.foodchem.2022.132589

Fasolin, L. H., Martins, A. J., Cerqueira, M. A., & Vicente, A. A. (2021). Modulating process parameters to change physical properties of bigels for food applications. *Food Structure, 28*, Article 100173. https://doi.org/10.1016/j.foostr.2020.100173

Francavilla, A., Corradini, M. G., & Joye, I. J. (2023). Bigels as delivery systems: Potential uses and applicability in food. *Gels, 9*(8), 648. https://doi.org/10.3390/gels9080648

Ghiasi, F., & Golmakani, M.-T. (2022). Fabrication and characterization of a novel biphasic system based on starch and ethylcellulose as an alternative fat replacer in a model food system. *Innovative Food Science & Emerging Technologies, 78*, Article 103028. https://doi.org/10.1016/j.ifset.2022.103028

Gonçalves, R. F. S., Martins, J. T., Abrunhosa, L., Baixinho, J., Matias, A. A., Vicente, A. A., & Pinheiro, A. C. (2021). Lipid-based nanostructures as a strategy to enhance curcumin bioaccessibility: Behavior under digestion and cytotoxicity assessment. *Food Research International, 143*, Article e110278. https://doi.org/10.1016/J.FOODRES.2021.110278

Jiménez-Munoz, L., Tsochatzis, E. D., & Corredig, M. (2022). Impact of the structural modifications of potato protein in the digestibility process under semi-dynamic simulated human gastrointestinal in vitro system. *Nutrients, 14*(12), 2505. https://doi.org/10.3390/nu14122505

Katzav, H., Chirug, L., Okun, Z., Davidovich-Pinhas, M., & Shpigelman, A. (2020). Comparison of thermal and high-pressure gelation of potato protein isolates. *Foods, 9*(8), 1041. https://doi.org/10.3390/foods9081041

Liu, W., Wang, J., McClements, D. J., & Zou, L. (2018). Encapsulation of β-carotene-loaded oil droplets in caseinate/alginate microparticles: Enhancement of carotenoid stability and bioaccessibility. *Journal of Functional Foods, 40*, 527–535. https://doi.org/10.1016/j.jff.2017.11.046

Lu, Y., Zhong, Y., Guo, X., Zhang, J., Gao, Y., & Mao, L. (2022). Structural modification of O/W bigels by glycerol monostearate for improved Co-delivery of curcumin and epigallocatechin gallate. *ACS Food Science and Technology, 2*(6), 975–983. https://doi.org/10.1021/ACSFOODSCITECH.2C00044/ASSET/IMAGES/LARGE/FS2C00044_0008.JPEG

Lupi, F. R., De Santo, M. P., Ciuchi, F., Baldino, N., & Gabriele, D. (2017). A rheological modelling and microscopic analysis of bigels. *Rheologica Acta, 56*(9), 753–763. https://doi.org/10.1007/s00397-017-1030-3

Machado, M., Sousa, S., Morais, P., Miranda, A., Rodriguez-Alcalá, L. M., Gomes, A. M., & Pintado, M. (2022). Novel avocado oil-functionalized yogurt with anti-obesity potential: Technological and nutraceutical perspectives. *Food Bioscience, 50*, Article 101983. https://doi.org/10.1016/j.fbio.2022.101983

Martín-Illana, A., Notario-Pérez, F., Cazorla-Luna, R., Ruiz-Caro, R., Bonferoni, M. C., Tamayo, A., & Veiga, M. D. (2022). Bigels as drug delivery systems: From their components to their applications. *Drug Discovery Today, 27*(4), 1008–1026. https://doi.org/10.1016/j.drudis.2021.12.011

Martinez, R. M., Magalhães, W. V., Sufi, B. da S., Padovani, G., Nazato, L. I. S., Velasco, M. V. R., Lannes, S. C. da S., & Baby, A. R. (2021). Vitamin E-loaded bigels and emulsions: Physicochemical characterization and potential biological application. *Colloids and Surfaces B: Biointerfaces, 201*, Article 111651. https://doi.org/10.1016/j.colsurfb.2021.111651

Martins, A. J., Guimarães, A., Fuciños, P., Sousa, P., Venâncio, A., Pastrana, L. M., & Cerqueira, M. A. (2023). Food-grade bigels: Evaluation of hydrogel:oleogel ratio and gelator concentration on their physicochemical properties. *Food Hydrocolloids, 143*, Article 108893. https://doi.org/10.1016/J.FOODHYD.2023.108893

Nutter, J., Shi, X., Lamsal, B., & Acevedo, N. C. (2023). Designing and characterizing multicomponent, plant-based bigels of rice bran wax, gums, and monoglycerides. *Food Hydrocolloids, 138*, Article 108425. https://doi.org/10.1016/j.foodhyd.2022.108425

Okonkwo, C. E., Ofoedu, C. E., Hussain, S. Z., Adeyanju, A. A., Naseer, B., Inyinbor, A. A., Olaniran, A. F., & Kamal-Eldin, A. (2022). Application of biogels for bioactives delivery: Recent developments and future research insights. *Applied Food Research, 2*(2), Article 100238. https://doi.org/10.1016/j.afres.2022.100238

Quilaqueo, M., Iturra, N., Contardo, I., Millao, S., Morales, E., & Rubilar, M. (2022). Food-grade bigels with potential to replace saturated and trans fats in cookies. *Gels, 8*(7), 445. https://doi.org/10.3390/gels8070445

Ryu, J., & McClements, D. J. (2024). Impact of heat-set and cold-set gelling polysaccharides on potato protein gelation: Gellan gum, agar, and methylcellulose. Food Hydrocolloids, 149, 109535. https://doi.org/10.1016/J.FOODHYD.2023.109535.

Ryu, J., Xiang, X., Hu, X., Rosenfeld, S. E., Qin, D., Zhou, H., & McClements, D. J. (2023). Assembly of plant-based meat analogs using soft matter physics: A coacervation-shearing-gelation approach. *Food Hydrocolloids, 142*, Article 108817. https://doi.org/10.1016/J.FOODHYD.2023.108817

Shakeel, A., Farooq, U., Gabriele, D., Marangoni, A. G., & Lupi, F. R. (2021). Bigels and multi-component organogels: An overview from rheological perspective. *Food Hydrocolloids, 111*, Article 106190. https://doi.org/10.1016/j.foodhyd.2020.106190

Shakeel, A., Lupi, F. R., Gabriele, D., Baldino, N., & De Cindio, B. (2018). Bigels: A unique class of materials for drug delivery applications. *Soft Materials, 16*(2), 77–93. https://doi.org/10.1080/1539445X.2018.1424638

Tan, Y., & McClements, D. J. (2021). Plant-based colloidal delivery systems for bioactives. *Molecules, 26*(22), 6895. https://doi.org/10.3390/molecules26226895

Tan, Y., Wannasin, D., & McClements, D. J. (2023). Utilization of potato protein fractions to form oil-in-water nanoemulsions: Impact of pH, salt, and heat on their stability. *Food Hydrocolloids, 137*, Article 108356. https://doi.org/10.1016/j.foodhyd.2022.108356

Wu, Y., Mou, B., Song, S., Tan, C.-P., Lai, O.-M., Shen, C., & Cheong, L.-Z. (2020). Curcumin-loaded liposomes prepared from bovine milk and krill phospholipids: Effects of chemical composition on storage stability, in-vitro digestibility and anti-hyperglycemic properties. *Food Research International, 136*, Article 109301. https://doi.org/10.1016/j.foodres.2020.109301

Xie, D., Hu, H., Huang, Q., & Lu, X. (2023). Development and characterization of food-grade bigel system for 3D printing applications: Role of oleogel/hydrogel ratios and emulsifiers. *Food Hydrocolloids, 139*, Article 108565. https://doi.org/10.1016/j.foodhyd.2023.108565

Yang, J., Fu, Y., Zheng, H., Jia, Y., Gao, Y., Yin, S., & Mao, L. (2023). Structural design of oleogel-hydrogel bigels for Co-delivery of curcumin and epigallocatechin gallate with synergistic stability and bioactivity. *Advanced Materials Technologies, 8*(14), Article 2202185. https://doi.org/10.1002/admt.202202185

Yang, J., Zheng, H., Mo, Y., Gao, Y., & Mao, L. (2022). Structural characterization of hydrogel-oleogel biphasic systems as affected by oleogelators. *Food Research International, 158*, Article 111536. https://doi.org/10.1016/j.foodres.2022.111536

Zampouni, K., Mouzakitis, C. K., Lazaridou, A., Moschakis, T., & Katsanidis, E. (2023). Physicochemical properties and microstructure of bigels formed with gelatin and κ-carrageenan hydrogels and monoglycerides in olive oil oleogels. *Food Hydrocolloids, 140*, Article 108636. https://doi.org/10.1016/j.foodhyd.2023.108636

Zhang, Z., Zhang, R., Zou, L., Chen, L., Ahmed, Y., Al Bishri, W., Balamash, K., & McClements, D. J. (2016). Encapsulation of curcumin in polysaccharide-based hydrogel beads: Impact of bead type on lipid digestion and curcumin bioaccessibility. *Food Hydrocolloids, 58*, 160–170. https://doi.org/10.1016/j.foodhyd.2016.02.036

Zheng, R., Chen, Y., Wang, Y., Rogers, M. A., Cao, Y., & Lan, Y. (2023). Microstructure and physical properties of novel bigel-based foamed emulsions. *Food Hydrocolloids, 134*, Article 108097. https://doi.org/10.1016/j.foodhyd.2022.108097

Zheng, H., Mao, L., Cui, M., Liu, J., & Gao, Y. (2020). Development of food-grade bigels based on κ-carrageenan hydrogel and monoglyceride oleogels as carriers for β-carotene: Roles of oleogel fraction. *Food Hydrocolloids, 105*, Article 105855. https://doi.org/10.1016/j.foodhyd.2020.105855

Zhou, H., Hu, X., Xiang, X., & McClements, D. J. (2023). Modification of textural attributes of potato protein gels using salts, polysaccharides, and transglutaminase: Development of plant-based foods. *Food Hydrocolloids, 144*, Article 108909. https://doi.org/10.1016/J.FOODHYD.2023.108909

Zhu, Q., Gao, J., Han, L., Han, K., Wei, W., Wu, T., Li, J., & Zhang, M. (2021). Development and characterization of novel bigels based on monoglyceride-beeswax oleogel and high acyl gellan gum hydrogel for lycopene delivery. *Food Chemistry, 365*, Article 130419. https://doi.org/10.1016/j.foodchem.2021.130419